AD_____

AWARD NUMBER: DAMD17-03-1-0368

TITLE: Fluorescent Immunoassay Development for PrPSc Detection and Antemortem Diagnosis of TSEs

PRINCIPAL INVESTIGATOR: Richard I. Carp, V.M.D., Ph.D.

CONTRACTING ORGANIZATION: The Research Foundation of SUNY
Brooklyn, New York 11203-3205

REPORT DATE: October 2005

TYPE OF REPORT: Annual

PREPARED FOR: U.S. Army Medical Research and Materiel Command
Fort Detrick, Maryland 21702-5012

REPORT DOCUMENTATION PAGE

Form Approved
OMB No. 0704-0188

1. REPORT DATE *(DD-MM-YYYY)*	**2. REPORT TYPE**	**3. DATES COVERED** *(From - To)*
01-10-2005	Annual	30 Sep 2004 – 29 Sep 2005

4. TITLE AND SUBTITLE

Fluorescent Immunoassay Development for PrPSc Detection and Antemortem Diagnosis of TSEs

5a. CONTRACT NUMBER

5b. GRANT NUMBER
DAMD17-03-1-0368

5c. PROGRAM ELEMENT NUMBER

6. AUTHOR(S)

Richard I. Carp, V.M.D., Ph.D.

E-Mail: richard.carp@omr.state.ny.us

5d. PROJECT NUMBER

5e. TASK NUMBER

5f. WORK UNIT NUMBER

7. PERFORMING ORGANIZATION NAME(S) AND ADDRESS(ES)

The Research Foundation of SUNY
Brooklyn, New York 11203-3205

8. PERFORMING ORGANIZATION REPORT NUMBER

9. SPONSORING / MONITORING AGENCY NAME(S) AND ADDRESS(ES)
U.S. Army Medical Research and Materiel Command
Fort Detrick, Maryland 21702-5012

10. SPONSOR/MONITOR'S ACRONYM(S)

11. SPONSOR/MONITOR'S REPORT NUMBER(S)

12. DISTRIBUTION / AVAILABILITY STATEMENT
Approved for Public Release; Distribution Unlimited

13. SUPPLEMENTARY NOTES

14. ABSTRACT

The overall goal of our study is to develop methods of high-sensitivity and high-specificity for the antemortem diagnosis of prion diseases by detecting PrPSc in biological fluids using fluorescent immunoassay. During the second year of this contract, we have focused on the development of an immunological method to isolate blood PrP from normal and scrapie-infected animals and the assembly of an optical fiber-based fluorescence detection system. By using magnetic beds-based immunocapture protocols, plasma PrP from normal and scrapie-infected animals was successfully isolated and can be detected directly by Western blot. In terms of the resistance of PrP to proteinase K (PK) digestion, there was no marked difference in plasma PrPs between normal and infected animals although more extensive conditions should be tested. For instrumentation, the design and assembly of an optical fiber-based fluorescence detection system for use with immunoassays for PrP is completed. The key features of the detection system are maximum light collection efficiency through the use of 4π steradian collection for the detectors, sampling of the entire sample volume through axial excitation with one or more lasers, and small sample volume, appropriate for assay work on TSEs. In addition to this, the system is designed for ease of use by employing disposable micro-capillaries as a sample holder.

15. SUBJECT TERMS
immunoassay, blood plasma PrP, optical fiber-based fluorescence detection system

16. SECURITY CLASSIFICATION OF:			**17. LIMITATION OF ABSTRACT**	**18. NUMBER OF PAGES**	**19a. NAME OF RESPONSIBLE PERSON**
a. REPORT	**b. ABSTRACT**	**c. THIS PAGE**			**19b. TELEPHONE NUMBER** *(include area code)*
U	U	U	UU	18	USAMRMC

Standard Form 298 (Rev. 8-98)
Prescribed by ANSI Std. Z39.18

Table of Contents

Introduction

The overall goal of our study is to develop methods of high-sensitivity and high-specificity for the antemortem diagnosis of prion diseases by detecting PrP^{Sc} in biological fluids using fluorescent immunoassay. To achieve our goal, we have focused on: (1) development of an immunological method to isolate blood PrP from normal and scrapie-infected animals, (2) discrimination of purified PrPs from the blood of normal and scrapie-infected animals by differential PK digestion, (3) immunization of mice with AGE-modified PrP peptides mixed with CpG oligonucleotides, (4) modifications to the existing LIF spectrofluorometer, (5) design and assembly of a optical fiber-based fluorescence detection system.

Body

1. Immunoprecipitation of PrP^{C} and PrP^{Sc} from the brains of normal and 263K-infected hamsters

For use in immunoprecipitation (IP), magnetic beads (M-280 Dynabeads, Dynal) coated with anti-PrP monoclonal antibody (mAb), 3F4 (Kascsak et al., 1987) or 4C4 (Kim et al., 2005), were prepared according to the manufacturer's instruction. The 10% brain homogenates (w/v) were prepared in IP buffer (100 mM NaCl/10 mM EDTA/0.5% Nonidet P-40/0.5% sodium deoxycholate/10 mM Tris-HCl, pH 7.5), followed by centrifugation at 3,000 × *g* for 10 min at 4°C to remove debris. Brain homogenate was divided into two aliquots: one untreated and another treated with 100 ug/ml of PK (Sigma-Aldrich, St. Louis, MO, USA) for 10 min at 37°C followed by protease inhibitor cocktails containing Pefabloc SC (Roche, Indianapolis, IN, USA) and Complete Mini (Roche, Indianapolis, IN, USA).

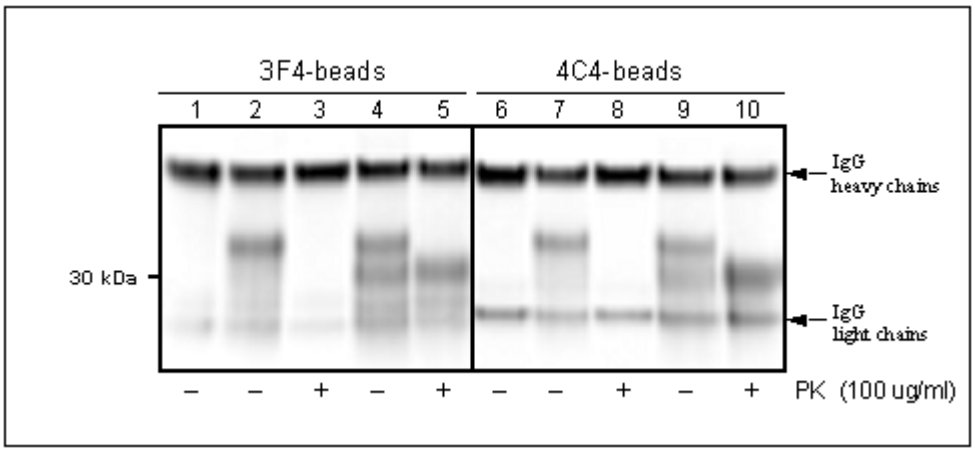

Figure 1. Western blot analysis of immunoprecipitated PrP using anti-PrP mAb-coated magnetic beads. Thirty ul of normal (n=3) and 263K-infected hamster (n=3) brain homogenates without or with PK treatment (100 ug/ml for 10 min at 37°C) were used for immunoprecipitation. As a negative control, blank sample lacking brain homogenate was included. Immune-complex captured on the beads were eluted with 2× SDS sample buffer and analyzed by SDS-PAGE (8-16% gradient gel) and Western blot using mAb 3F4. Lanes 1 & 6: negative control containing no brain material, lanes 2, 3, 7, 8: normal hamster brain homogenates, lanes 4, 5, 9, 10: 263K-infected hamster brain homogenates.

Immunoprecipitation (IP) was then performed as described (Kim et al., 2005) by using 30 ul of clarified homogenate and 3F4- or 4C4-conjugated beads (10 ug of mAb/6 $\times 10^7$ beads) in 300 ul of IP buffer. After incubation with constant mixing for 1.5 h at room temperature, the beads were attracted to the sidewall of the plastic tubes by external magnetic force, allowing easy removal of all unbound materials in the solution. After three washes in wash buffer (TBS containing 0.1% Tween-20), the beads were collected and were heated at 95°C for 5 min in SDS sample buffer and analyzed by SDS-PAGE (8-16% gradient gel) and Western blot using mAb 3F4.

Western blot analysis of the eluates is shown in Fig. 1. Regardless of the anitibody used to coat the beads, PK-resistant PrP^{Sc} was detected only in PK-treated brain homogenates of 263K-infected hamsters (Fig. 1B, lanes 5 & 10). Heavy or light chains of IgG were observed not only in samples with PrP (Fig. 1B, lanes 2, 4, 5, 7, 9, and 10) but also in those without PrP (Fig. 1B, lanes 1, 3, 6, and 8). The IgG signals from non-PrP containing samples are derived from the partial co-elution of the mAbs from the beads. From this result, we confirmed that PrP^{C} and PrP^{Sc} from normal and 263K-

infected hamster brains could be efficiently isolated with anti-PrP mAb-conjugated beads.

2. Isolation and detection of blood PrP from normal and 263K-infected hamsters

To test the applicability of the current IP protocol to the detection of PrP in blood samples, we performed IP of PrP from normal and 263K-infected hamster plasma using 4C4-coated magnetic beads. Plasma was isolated from heparinized blood of normal and infected hamsters by centrifugation at 4,000 × g for 15 minutes at room temperature. Some plasma samples were treated with or without PK (100 ug/ml for 10 min at 37°C). One ml of plasma was diluted in 9 ml of IP buffer. Fifty ul of 4C4-coated beads (50 ug of mAb) were added to the mixture and incubated for 1.5 hrs at room temperature. As a positive control for immunoprecipitation of PrP, 1 ml of 10% 263K hamster brain homogenates treated with or without PK was used. After extensive washing with PBS containing 0.1% Tween-20, bound material was eluted from the beads by heating at 99°C for 5 min in 2× SDS-PAGE sample buffer. Eluted samples were separated on 12% SDS-PAGE and analyzed by Western blot using biotin-7A12 (Zanusso et al., 1998; Li et al., 2000) as a primary antibody.

From 263K-infected brain as positive controls, large amounts of PrP^{Sc} were obtained (Fig. 2, lanes 3 & 4). In the absence of PK treatment, strong PrP bands ranging Mw 28-35 kDa were detected from normal and 263K plasma samples (Fig. 2, lanes 5 & 7, respectively). These PrP signals disappeared after 100 ug/ml PK pretreatment. Since biotinylated anti-PrP mAb 7A12 and streptavidin-conjugated HRP were used for Western blot, the PrP bands detected can not be resulted from a non-specific binding of secondary antibody to partially co-eluted IgG from the beads. To further verify the identity of the PrP bands, we also included the blot treated only with secondary HRP-conjugate (Fig. 2, lower panel), in which no non-specific signals were observed.

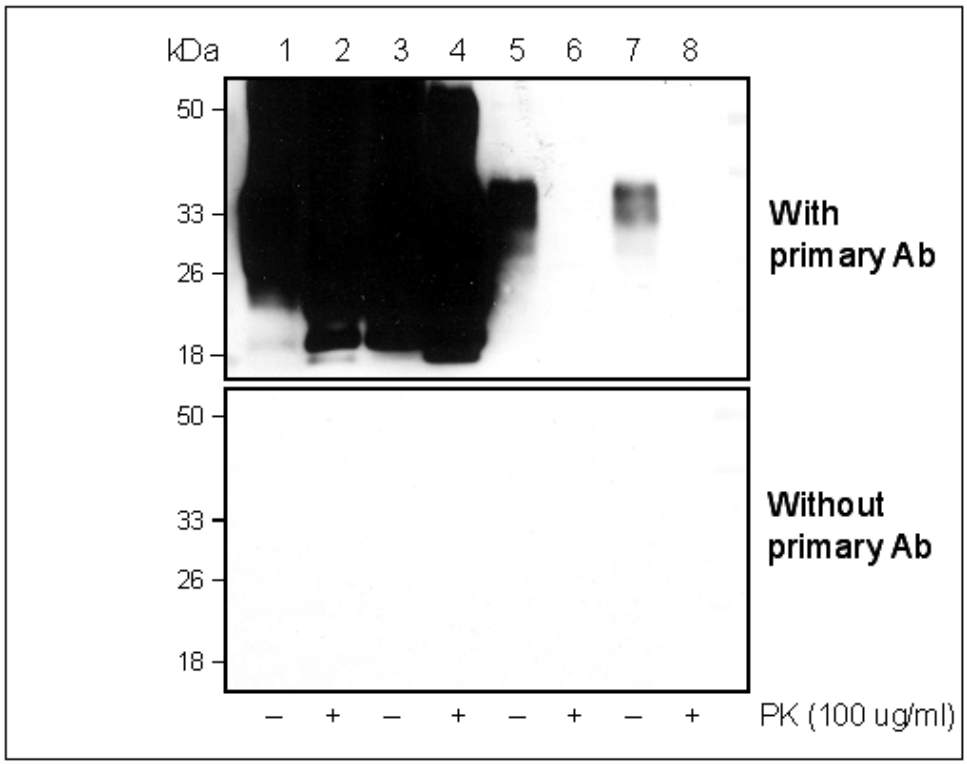

Figure 2. Immunoprecipitation of plasma PrP from normal and 263K-infected hamsters. One ml of plasma from normal and 263K-infected hamster without or with PK treatment (100 ug/ml for 10 min at 37^{o}C) was used for immunoprecipitation. As positive controls, approximately 1 ug of purified 263K/PrP^{Sc} was processed by the same procedure as that used for plasma samples. Immune-complex captured on the beads were eluted with 2× SDS sample buffer and analyzed by 12% SDS-PAGE and Western blot using biotin-7A12. Lanes 1 & 2: 263K brain homogenates as positive controls for Western blot, lanes, 3 & 4: purified 263K/PrP^{Sc} as positive controls for immunoprecipitation, lanes 5 & 6: plasma from normal hamster, lane 7 & 8: plasma from 263K-infected hamster. Lower panel: primary antibody (biotin-7A12) was omitted to test the specificity of the signals detected in the upper panel.

3. Isolation and detection of blood PrP from normal and sheep scrapie

For the detection of plasma PrP from normal and scrapie sheep, the same IP protocol as for hamster plasma was used. As shown in Fig. 3, intense PrP signals in the range of Mw 27-35 kDa were detected from normal and scrapie sheep (lanes 4 & 5, respectively). As positive controls for IP, normal and 263K hamster plasma samples were used (Fig. 3, lanes 2 & 3). These results indicate that IP protocol used in this study can be used for the isolation of plasma PrP from hamster as well as from sheep.

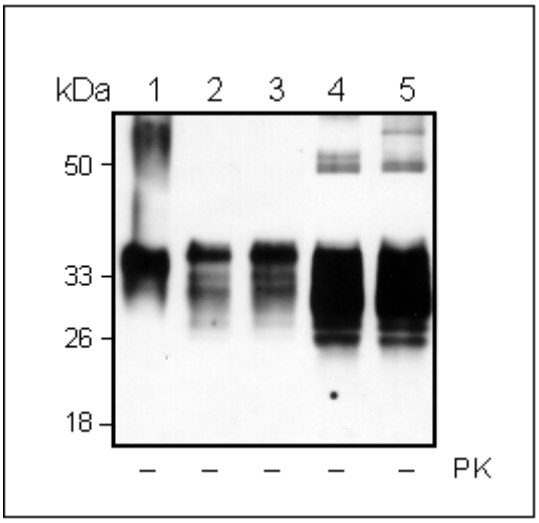

Figure 3. Immunoprecipitation of plasma PrP from normal and scrapie sheep. Except for PK treatment, refer to the legend in Fig. 2 for experimental protocol. As positive controls, approximately 1 ug of purified 263K/PrP^{Sc} was processed using the same protocol as that used for plasma samples. Immune-complex captured on the beads were eluted with 2× SDS sample buffer and analyzed by 12% SDS-PAGE and Western blot using biotin-7A12. Lane 1: 263K brain homogenates as positive control for Western blot, lanes 2 & 3: plasma from normal and 263K-infected hamster, respectively, as positive controls for IP, lanes 4 & 5: plasma from normal and scrapie sheep, respectively.

4. Treatment of plasma PrP with various concentrations of PK

To examine if there is any difference in PK resistance of plasma PrP from normal and 263K-infected hamster, samples were treated with various concentrations of PK ranging from 1 to 50 ug/ml for 10 min at 37°C. In this experiment, 500 ul of 0.1 M glycine (pH 2.8) per 1 ml of starting plasma sample was used as elution buffer instead of 2× SDS sample buffer. The eluate was neutralized by adding 1/20 volume of 1 M Tris (pH 9.5) and then concentrated to 20 ul of volume using Microcon centrifugal filter unit (NMWL; 10,000) (Millipore, USA). Prior to loading on the gel, purified plasma samples were treated without or with PK at various concentrations for 10 min and separated on 12 % SDS-PAGE. As shown in Fig. 4, regardless of PK concentration, all PrP bands from normal and 263K disappeared after digestion with PK.

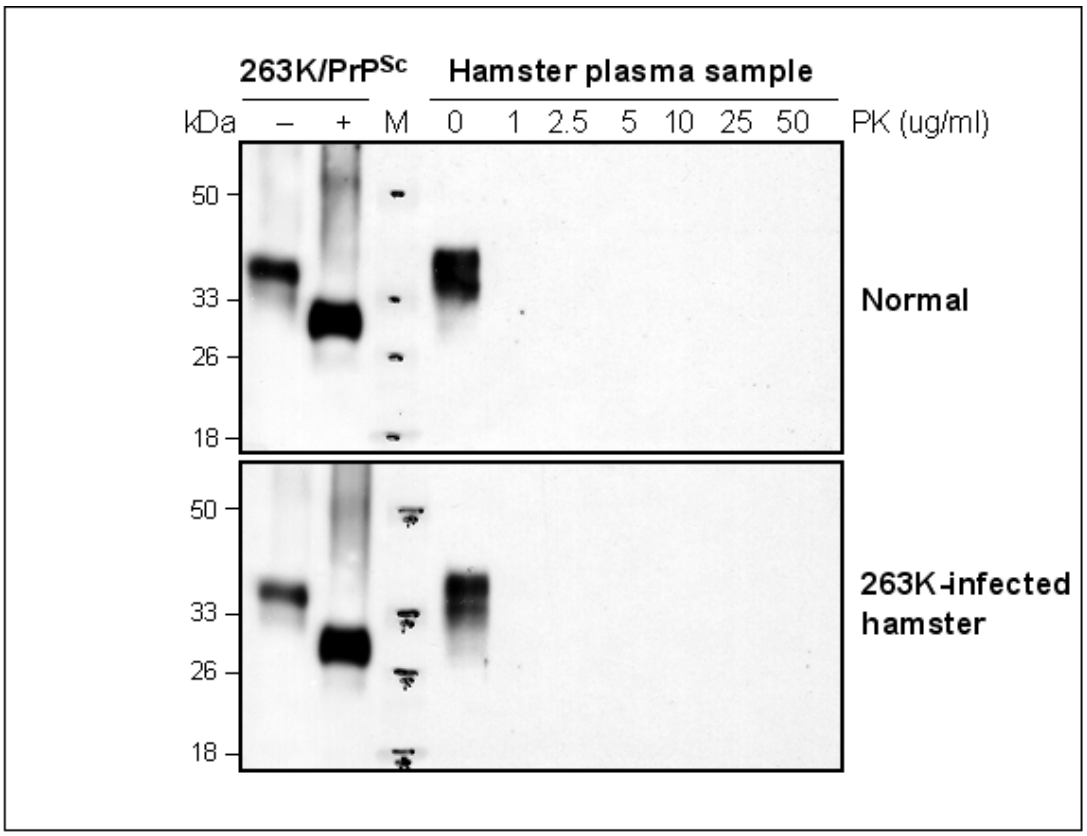

Figure 4. Treatment of plasma PrP from normal and 263K-infected hamsters with various concentrations of PK. Lanes 1 & 2: purified 263K/PrP^{Sc} from 263K hamster brain as positive controls for Western blot. Plasma PrP bands disappeared after digestion with various concentrations of PK. Biotin-7A12 was used as the primary Ab.

Although more extensive experiments are needed to optimize the conditions for the detection of blood PrP as well as for PK treatment, the present results appear to be promising because PrP in plasma from normal and TSE-affected animals could be detected by immunoprecipitation followed by Western blot. To our knowledge, there are no reports on the direct detection of blood PrP by Western blot. By animal bioassay using hamsters and transgenic mice harboring sheep PrP gene, we are testing the presence of TSE infectivity in the blood PrPs from 263K hamster and scrapie sheep, respectively. In addition, various characterization experiments are currently ongoing to further verify the identity of blood PrP as well as to find out any biochemical difference between plasma PrPs from normal and infected animals.

5. Immunization of mice with AGE-modified PrP peptides

AGE-modified PrP peptide 23-36 (KKRPKPGGWNTGGS) (designated AGE-PrP) was prepared as described previously (Choi et al., 2004). In addition, AGE-modified PrP 23-36 and BSA mixture (designated AGE-PrP-BSA) was prepared as well in order to prevent any failure in inducing the immune reaction against AGE-PrP 23-36 due to its small size as an immunogen. Briefly, PrP peptide or a mixture of BSA and PrP peptide was mixed with D-glucose and dissolved in 0.5 M sodium phosphate buffer (pH 7.4). The solutions were deoxygenated with nitrogen gas, sterilized by ultrafiltration (0.45-μ filter), and then incubated at 37°C for 90 days. After incubation, the samples were dialyzed using three changes of 20 mM sodium phosphate buffer (pH 7.4) containing 0.15 M NaCl. The dialyzed samples were lyophilized and then dissolved in sterilized distilled water at 1 mg/ml concentration.

Antigens were prepared for injection by emulsification with adjuvant CytRx (G-5 Titermax Gold, Titermax USA) as described by the manufacturer. Enough emulsified antigens were prepared each time to deliver 200 ul injection per mouse. PrP-knockout and Balb/C mice were immunized every three weeks by subcutaneous and intramuscular injections for a total of nine weeks. The mice also received 30 uL CpG oligodeoxynucleotide 1826 (synthesized by Integrated DNA Technologies Inc, Coralville, IA), which consists of a central unmethylated CpG dinucleotide flanked by two 5' purines and two 3' pyrimidines, and has been shown to be a strong inducer of innate immunity (Lipford et al., 1998; Sethi et al., 2002). One week after the final boost, the mice were bled retro-orbitally and the sera are currently being tested for reactivity against the antigen by ELISA and Western blot. The reactivity of polyclonal R3 Ab (Choi et al., 2004) will be used as a positive control.

6. Modifications to the Existing LIF Spectrofluorometer

During this year we replaced the helium-neon (He-Ne) laser in the fluorescence spectrometer with a small diode-pumped solid-state frequency-doubled, neodymium (Nd):YAG laser. There were several reasons for this change of lasers. First, and foremost, the doubled Nd:YAG laser's output is in the green region of the optical spectrum at a wavelength of 532 nm while that of the He-Ne laser is at 633nm. The

diode pumped Nd:YAG lasers are much smaller than the He-Ne lasers and are much more powerful while having higher efficiency. This implies that a 50mw Nd:YAG laser can easily replace the 15mw He-Ne laser with no penalty in power consumption or size. In fact, the second reason for changing the laser was that fluorescent dyes that are excited by green radiation usually have higher fluorescence quantum efficiency than do dyes developed for the red spectral region. Two minor changes of optical components were made, a beam splitter and an interference filter. The device was optically aligned and operated.

Table 1. Comparison of the dynamic range of LIF spectrofluorometer equipped with Nd:YAG laser

Dyes \ Conc. (nM)	5	5×10^{-1}	5×10^{-2}	5×10^{-3}	5×10^{-4}	5×10^{-5}	5×10^{-6}	0
Alexa-532[a]	13.00[#*]	3.14	1.26	1.10	1.12	1.07	1.07	1.05
B-PE[b]	13.00	13.00	6.49	1.60	1.14	1.09	1.08	1.05
R-PE4[c]	13.00	13.00	6.12	1.57	1.13	1.09	1.09	1.06
5-R-6G[d]	7.64	1.70	1.18	1.11	1.09	1.06	1.08	1.05
6-R-6G[e]	13.00	2.46	1.25	1.07	1.07	1.07	1.07	1.05
Qdot 655[f]	13.00	2.92	1.42	1.42	1.41	1.42	1.41	1.41

[#]Signal-to-baseline (S/B) ratio from various dilutions of dyes were analyzed by using LIF spectrofluorometer equipped with Nd:YAG laser as a light source. The S/B ratio from the dyes in PBS was measured for 0.5 sec with 0.1 sec integration time and the value above the cutoff sensitivity for each dye is marked with gray shading.
*S/B ratio larger than 13.00 is out of the dynamic range of the spectrofluorometer.
[a]AlexaFluor 532 (M*r* 1,200; Ex 530 nm/Em 554 nm; ε=81,000 cm^{-1} M^{-1})
[b]B-Phycoerythrin (M*r* 240,000; Ex 546, 565 nm/Em 575 nm; ε=2,410,000 cm^{-1} M^{-1})
[c]R-Phycoerythrin (M*r* 240,000; Ex 480, 546, 565 nm/Em 578 nm; ε=1,960,000 cm^{-1} M^{-1})
[d]5-Rhodamine 6G (M*r* 555.59; Ex 524 nm/Em 557 nm; ε=108,000 cm^{-1} M^{-1})
[e]6-Rhodamine 6G (M*r* 555.59; Ex 524 nm/Em 550 nm; ε=102,000 cm^{-1} M^{-1})
[f]Quantum Dot 655 (M*r* 100,000; Ex <600 nm/Em 654 nm; ε>1,000,000 cm^{-1} M^{-1})

To check whether there was any improvement in the sensitivity of the instrument after replacement of the light source, we have analyzed the dynamic range of the spectrofluorometer using serial dilutions of various fluorescent dyes (0 – 5 nM) compatible with Nd:YAG laser (Table 1). Most prominent amongst these was PE: detection limits for both B-PE and R-PE were between 5×10^{-5} and 5×10^{-4} nM (Table 1).

As previously reported (Kim et al., 2005), the lowest amount of Alexa Fluor 633 dye that can be detected by the fluorometer equipped with He-Ne laser was between 5×10^{-6} and 5×10^{-5} nM. This comparative result indicates that the replacement of the light source only was not effective in terms of the sensitivity improvement. The current instrument is designed for high spectral resolution, employing a back-thinned thermoelectrically cooled CCD (Rubenstein et al., 2003). While this detector has high sensitivity (appropriate for its use as a high spectral resolution instrument) it has relatively low gain compared to avalanche diodes or photo-multiplier tubes. To increase the sensitivity of the LIF spectrofluorometer we are currently exploring the use of avalanche diodes or photo-multiplies tubes detectors in conjunction with Nd:YAG laser. We will continue to refine the optical system as well in order to achieve the higher sensitivity that is expected.

7. Fiber Based Fluorescence Detection

A major component of the experimental activity for this proposal is to drive the sensitivity of detection of PrP in blood or urine, with as little sample preparation as possible. With sufficient sensitivity, high throughput analysis would be possible making a whole range of previously not achievable experimental designs available. The high end estimates for concentration of PrP^{Sc} in blood (femptomolar, Brown et. al.) show that detection would be necessary of a few tens of millions of molecules. This is not an unreasonable number of molecules, and well within the reach of current laser fluorescence techniques (see below). Our approach to this problem will be to start with a fiber optic based, small volume (1-100 μl), detection system, designed to capture maximal amount of fluorescence signal, and develop ever increasingly sensitive detection methods as the problem requires. We will start with photo voltaic and avalanche diode detectors and CW excitation, and transition to short pulse laser detection capable of single molecule sensitivity. This later technique should allow us to leverage off existing immuno-fluorescence assays to detection levels limited by non-specific binding.

We have designed and constructed[1] a unique fiber optical assembly that can be used for ultra sensitive, laser-induced fluorescence detection of PrP, shown in Fig. 5. The ‘cross’ assembly consists of bundles of optical fibers which feed from a detector mounted at the end of each arm to each side of a block drilled to accept a micro-capillary. We have

started with 100 and 50 microliter capillaries, but sample size can be adjusted by switching out the capillary holder block. The device makes use of an array of 180 optical fibers which are optically coupled to a 50 microliter capillary sample tube. The close proximity of each of the fiber ends to the walls of the capillary as well as the large acceptance angle (28 degrees) of each fiber $(NA=.25)^2$ make the light collection efficiency of the array nearly 100 percent. The 180 fibers in the array are divided into four linear assemblies of 45 fibers each which are vertically stacked, cemented into a sturdy unit and located at 90 degree intervals around the central capillary holder. Each of these sets of 45 fibers are collected, potted in epoxy and are brought to a polished end which is close-coupled to a sensitive silicon photo diode or vacuum photomultiplier through appropriate optical filtration. The excitation laser is brought into the sample capillary either through the open top or bottom of the capillary in this manner. The fluorescent signal from each arm of the array is then processed by electronics that can discriminate against common-mode noise, ensuring the highest level of signal to noise. This permits the measurement of fluorescence at extraordinarily high dilution levels, where dyes are used, or at very low concentrations of PrP.

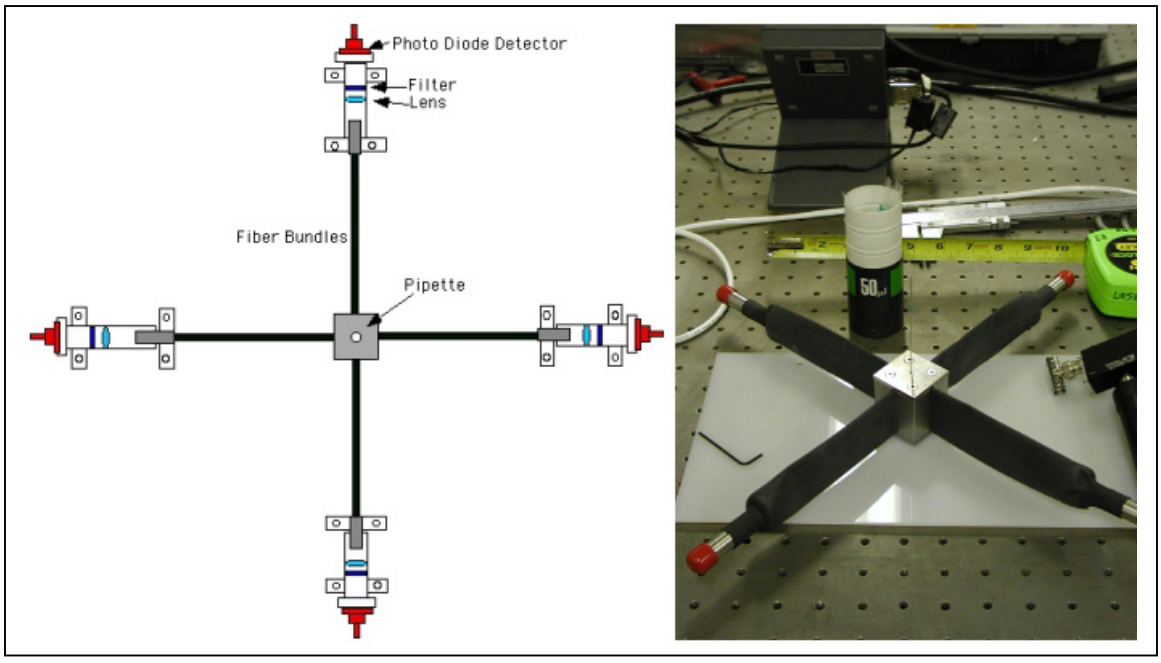

Fig. 5. Fiber based detector head, bundles of optical fibers surround a target (Drummond micro-capillary) allowing for 4π steradian detection of signal from axial laser excitation of the sample.

The mounted fiber detector head is shown in Fig. 6. An aluminum base plate has been designed and machined to support the fiber ‘cross’ assembly. The plate supports the individual detectors at the end of each bundle of fibers as well as the sample block, located in the center of the plate. This configuration is designed to assure that there is no stress on the optical fiber bundles. The plate is drilled to allow introduction of the capillary through the back of the plate. In the final configuration for the instrument, this will be the top and a sample cover, which is interlocked to the laser excitation source, will make the instrument a class I laser device. During test and evaluation we have mounted the lasers externally to the system (photograph on right). In the final system lasers will be mounted on a separate plate and directed through the sample slit by means of a turning mirror, as seen in the diagram on the left. The final instrument will be turn-key and have a footprint of approximately 18” x 18” x 4”. The sample will be loaded in a capillary tube, inserted into the slot and the cover dropped to make the measurement.

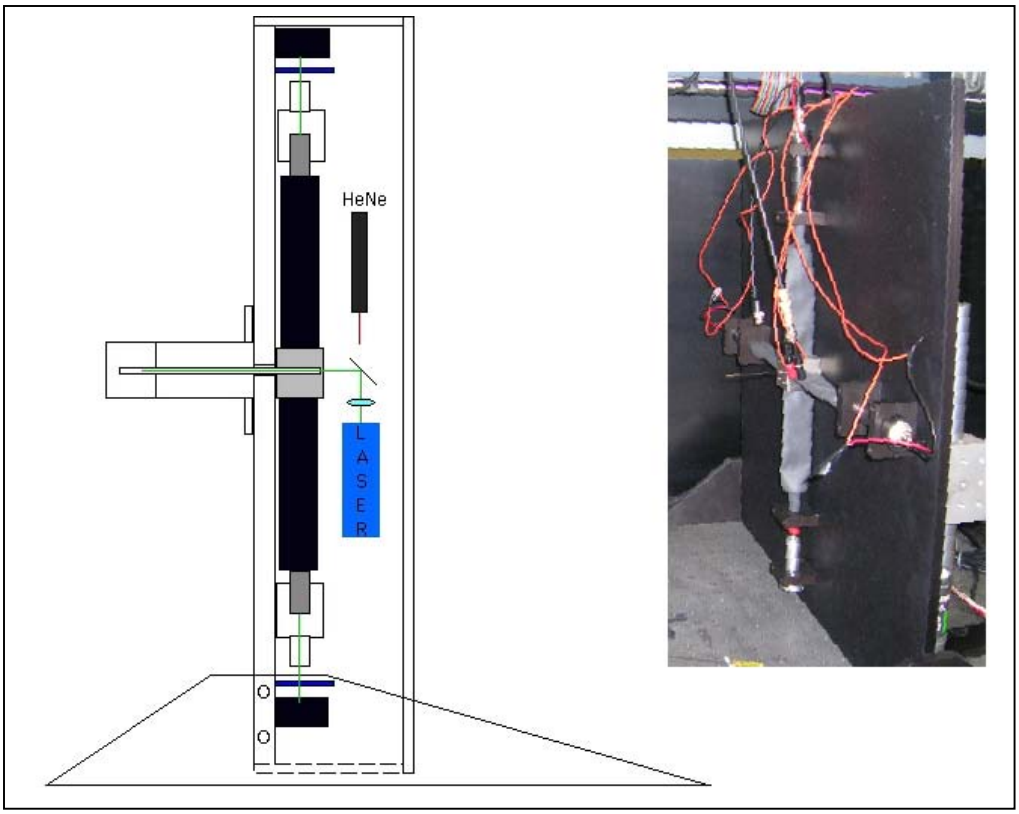

Fig. 6. Fiber mounting system. The fiber and detectors are supported by a base plate, which is drilled to accept the capillary sample from the back side. The lasers illuminate the sample along its axis. Final system will be mounted

The advantages of such a detection array are numerous. Primarily, it permits the use of very small samples at low concentration to be optimally interrogated using the short pulse laser, single molecule detection schemes, as described below. The multi-port geometry of the system allows efficient electronic processing of the signals from each arm of the device. Finally, and perhaps most important, since fiber optical cables are essentially lossless for optical transmission (attenuation less than 10db per kilometer)[3], once deployed for use in a BSL3 facility only the capillary assembly needs to be located in the facility, as the fluorescence information can be ported to a remote location where data processing and analysis can be accomplished.

This fiber based detection system is adaptable to existing short pulsed detection hardware, originally developed for sequencing of single DNA molecules, at LANL. By employing this detection scheme for collection of fluorescence we will be able to drive the sensitivity to the single molecule level, if necessary.

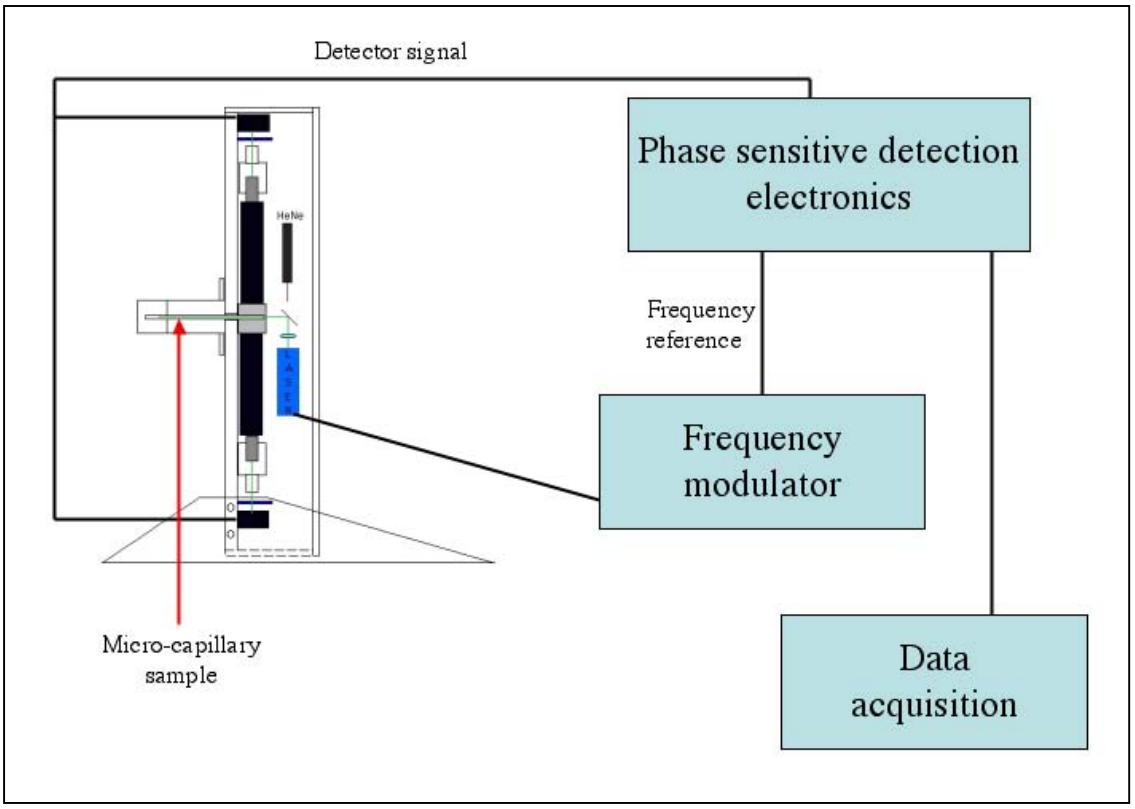

Fig. 7. Block diagram of detection electronics for fiber based detection system. Excitation source is frequency modulated for phase sensitive detection

Key Research Accomplishments

1. Blood plasma PrP from normal and TSE-affected animals was successfully isolated by magnetic beads-based immunocapture protocols and can be detected directly by Western blot.
2. The design and assembly of an optical fiber-based fluorescence detection system for use with immunoassays for PrP is completed.

Reportable Outcomes

None.

Conclusions

The work during the second year of this contract has provided important advancement in our capacity for the direct detection of blood PrP from normal and scrapie-infected animals. For instrumentation, the design and assembly of an optical fiber-based fluorescence detection system for use with immunoassays for PrP is completed. Improvements in both the biological and hardware areas have been made; this will further our efforts toward the goal of a fluorescent immunoassay system using a laser-induced fluorescence spectrofluorometer.

References

Choi YG, Kim JI, Jeon YC, Park SJ, Choi EK, Rubenstein R, Kascsak RJ, Carp RI, Kim YS. 2004. Nonenzymatic glycation at the N terminus of pathogenic prion protein in transmissible spongiform encephalopathies. J Biol Chem. 279: 30402-30409.

Kascsak RJ, Rubenstein R, Merz PA, Tonna-DeMasi M, Fersko R, Carp RI, Wisniewski HM, Diringer H. 1987. Mouse polyclonal and monoclonal antibody to scrapie-associated fibril proteins. J Virol. 61: 3688-3693.

Kim,JI, Wang C, Kuizon S, Xu J, Barengolts D, Gray PC, Rubenstein R. 2005. Simple and specific detection of abnormal prion protein by a magnetic bead-based immunoassay coupled with laser-induced fluorescence spectrofluorometry. J Neuroimmunol. 158: 112-119.

Li R, Liu T, Wong BS, Pan T, Morillas M, Swietnicki W, O'Rourke K, Gambetti P, Surewicz WK, Sy MS. 2000. Identification of an epitope in the C terminus of normal prion protein whose expression is modulated by binding events in the N terminus. J Mol Biol. 301: 567-573.

Lipford BG, Heeg K, Wagner H. 1998. Bacterial DNA as immune cell activator. Trends Microbiol. 6: 496–500.

Rubenstein R, Gray PC, Kim JI, Gary T, 2003. Diagnosis of prion diseases by multispectral techniques. In: Nunnally, B. & Krull, I.S. (Eds.), Prions and Mad Cow Disease, Marcel Dekker, New York. pp 333-358.

Sethi S, Lipford G, Wagner H, Kretzschmar H. 2002. Postexposure prophylaxis against prion disease with a stimulator of innate immunity. Lancet. 360: 229-230.

Zanusso G, Liu D, Ferrari S, Hegyi I, Yin X, Aguzzi A, Hornemann S, Liemann S, Glockshuber R, Manson JC, Brown P, Petersen RB, Gambetti P, Sy MS. 1998. Prion protein expression in different species: analysis with a panel of new mAbs.Proc Natl Acad Sci USA. 95: 8812-8816.

Polymicro Inc. Phoenix AZ

Polymicro Textbook of Fiber Optics, pg 2-4

IBID, pg 2-15

Appendices

None.